

Received March 26, 2020, accepted April 14, 2020, date of publication April 17, 2020, date of current version April 30, 2020.

Digital Object Identifier 10.1109/ACCESS.2020.2988530

# Multi-Objective Economic Scheduling of a Shipboard Microgrid Based on Self-Adaptive Collective Intelligence DE Algorithm

JINHONG FENG<sup>ID</sup>, JUNDONG ZHANG<sup>ID</sup>, CHUAN WANG<sup>ID</sup>, RUIZHENG JIANG<sup>ID</sup>, AND MINGYI XU

Marine Engineering College, Dalian Maritime University, Dalian 116026, China

Corresponding author: Jinhong Feng (fjhdlmu@dlmu.edu.cn)

This work was supported in part by the Natural Science Foundation of China under Contract 51709027.

**ABSTRACT** With the growing demand for emission reductions and fuel efficiency improvements, alternative energy sources and energy storage technologies are becoming popular in a ship microgrid. In order to balance the two non-compatible objectives, a new differential evolution variant, which is named as SaCIDE-*r*, was proposed to solve the optimization problem. In this algorithm, a Collective Intelligence (CI) based mutation operator was proposed by mixing some promising donor vectors in the current population. Besides, a self-adaptive mechanism which was developed to avoid introducing extra control parameters. Further, to avoid being trapped in local optima, a re-initialization mechanism was developed. Then, we have evaluated the performances of the proposed SaCIDE-*r* approach by studying some numerical optimization problems of Congress on Evolutionary Computation (CEC) 2013 with  $D = 30$ , compared with seven state-of-the-art DE algorithms. Moreover, the proposed SaCIDE-*r* method was applied for economic scheduling of a shipboard microgrid under different cases compared with other multi-objective optimizing methods, resulting in very competitive performances. The comprehensive experimental results have demonstrated that the presented SaCIDE-*r* method might be a feasible solution for such a kind of optimization problem.

**INDEX TERMS** Shipboard microgrid, global optimization, collective intelligence (CI), differential evolution (DE).

## I. INTRODUCTION

For most conventional cargo ships, in which Diesel Generators (DG) are the main power sources, DGs can be well controlled to meet the required power demands on board. Since 1997 stated in the International Convention for the Prevention of Pollution From Ships, which is usually shorten as MARPOL, by international maritime organization, minimizing operation costs and reducing gases emissions have become the main targets, which might be not compatible [1]. To meet the growing demands of the emission efficiency, power grids in conventional ships must be supplemented with some renewable sources such as Wind Turbines (WT), Photovoltaics (PV), battery system and fuel cells [2]–[4]. It is a central concept for such a hybrid microgrid to coordinately optimize the operations of DGs, PV, WT and batteries [5], [6]. For hybrid microgrids onboard, the islanded mode is the most

frequently used operation mode, and the interconnected mode is barely used. Among the renewable power sources, the PV generator is the most applicable for hybrid microgrids on board [7], [8]. Therefore, a shipboard microgrid mixing with PV, WT, battery and DG might be an feasible solution [8].

Many investigations have been conducted on such hybrid microgrids [9]–[13] by using HOMER software, which is a traditional tool for designing, optimizing and performance assessment of the hybrid power schemes. Nonetheless, there are some limitations in using this software which necessitate developing new approaches, and several optimization methods have been reported for sizing hybrid power schemes. Utilizing artificial intelligence is an appropriate approach to enhance the optimization process. Also, to overcome the problems related to using one method for optimization, hybrid optimization algorithms can be advantageous. In [14], the authors used a Clonal selection technique to optimize a hybrid solar and wind scheme with a battery to utilize its output with minimum cost and a small fluctuation rate. In [15],

The associate editor coordinating the review of this manuscript and approving it for publication was Wei-Chang Yeh<sup>ID</sup>.

the authors used an intelligent flower pollination algorithm to size optimally a hybrid system (solar/wind/hydrogen), minimizing the total life cycle cost. In [16], they investigated the effectiveness of Cuckoo Search in using a hybrid solar/wind/battery scheme design problem in an isolated area in India. Reference [17] Used the well-known heuristic methods based on simulated annealing (SA) for size optimization of a standalone PV-wind electrical system including a battery with minimum cost. The considered decision variables were as follows: capacity/size of WT, PV and battery (BAT). The authors found that the proposed method (SA) provides superior results relative to the other method. In another paper, the effect of using forecast load information instead of past information on the small independent hybrid power performance is investigated [18]. In [19], the sizing problem for a PV/WT/DG/fuel cell is solved by considering different hybrid systems and two scenarios related to the cost of the diesel fuel. Reference [20] Evaluated the performance of different evolutionary algorithms for optimum sizing of a PV/WT/battery hybrid system to continuously satisfy the load demand with the minimal total annual cost. In another paper, the size of the battery bank, the area of the photovoltaic system, and the fuel consumption of the diesel generator within the proposed hybrid system are optimized so as to minimize the life cycle cost of the system, and an efficient meta-heuristic technique based on tabu search is used [21]. In another research [22], the optimum sizing for a hybrid wind and solar energy system with energy storage was developed using a hybrid optimization algorithm based on Chaotic Search (CS) and Simulated Annealing (SA), namely, the hybrid search algorithm (HSA). The results are compared with those individually from the original Simulated Annealing and original Chaotic Search. These hybrid methods provide a new way for optimizing microgrids, showing some advantages and application prospects. Although the above investigations used various heuristic methods to solve the optimal sizing problem of hybrid power systems, the optimization objectives may not be suitable for shipboard microgrids. A shipboard hybrid microgrid is an isolated power grid with a very small size. In our study case, a microgrid in a barge consists of a PV (10kW), a WT (10kW), a DG (15kW) and a battery system (40kW). The max power of loads is not bigger than 12kW. For such a specific microgrid, loads usually vary according to the requirement of cargos and the ship owner with some randomness. Besides, a barge often locates at different anchorages. Thus, it is not feasible to evaluate the total annual cost for a shipboard microgrid. It seems to build up a more suitable optimizing modal for shipboard microgrids. On the other hand, the above methods are used to solve the optimization problem with single objective. Whereas, optimizing shipboard microgrids considering multi-objective need further investigations.

Compared with the various researches on hybrid microgrids land-based, it seems insufficient for investigations on optimizing microgrid of shipboards. In [23], the authors hybridized two types of energy storage systems and

proposed a two-step multi-objective optimization method for optimizing the management for all-electric ships. In [24], that investigation extended the principles of optimal planning and economic dispatch problems to shipboard systems by minimizing operating costs of DGs and energy storage systems. In [25], that paper focused on a parameter identification method for an electric model of a battery storage system on board. In [8], the authors presented the experimental results from the operation of a proto-type green ship. In [1], the investigation proposed an energy management system of the electrical system for a yacht to minimize fuel consumptions. Most of the existing researches have focus on the optimization of energy storage system and controllers, ignoring the overall schedule at shipboard microgrid level. Moreover, previous works rarely noticed that it is necessary to minimize the fuel cost and deterioration of the battery system for shipboard microgrids hybrid with PV, WT and DGs. Thus, it is necessary and significant to design an Energy Management Systems (EMS) which could satisfy multi-objective for such a shipboard hybrid microgrid.

Due to the complexity of scheduling microgrids considering efficiency and emission, many algorithms have been proposed to address this issue. In [26], a method which combined a real-coded Genetic Algorithm (GA) and a Mixed Integer Linear Programming (MILP) was proposed to schedule the economic dispatch of the microgrid. In [27], the authors proposed an adaptive nesting evolutionary algorithm to optimize the configuration and planning of a microgrid. In [28], the authors presented a two-stage robust optimal dispatch model for a representative islanded microgrid which mixed with Alternating Current (AC) and Direct Current (DC). In [29], that paper proposed a framework to conduct robust/stochastic optimization of a microgrid considering real and reactive power flow. The optimizing problem is a mixed integer nonlinear programming (MINLP) problem, which was solved by a software. In [30], the authors proposed a day-ahead economic scheduling of microgrid considering charging/discharging cycles of the battery system. And the objective functions were solved by using a hybrid method mixed with Particle Swarm Optimization (PSO), the Rainflow algorithm and scenario techniques. In [31], that paper proposed an approximate dynamic programming approach for the economic dispatch of a microgrid with distributed generators considering the uncertainties of stochastic variables. Although the above researchers have investigated this problem by using various algorithms, the performance of economic scheduling on board with multi-objectives is still not satisfying due to the complexity.

Differential Evolution (DE) has been well accepted as a easily-used but effective method in the family of Evolutionary Algorithm (EA) [32]. Over the past two decades, many variants [33]–[41] of DE have been developed to solve various engineering problems, such as optimal power flow [42], parameters identification [43], feature selection [44], railway line planning [45], wireless sensor network [46], optimal location of battery swapping stations [47], mild depressive

detection [48], path planning of mobile robots [49] and DC motor controller [50]. For DE algorithm, it is crucial to generate a new mutant vector for the final performance of the designed DE. In most cases, the mutant vectors come from randomly selected vectors or/and the best vector in the current population. Such a kind of mutation operator only uses a few individuals in the population. It is different from what has been observed in other engineering domains [51]. Meanwhile, it is also very important for DEs to avoid meeting a stagnation which means no better solutions generated [52]. To address these issues, we would like to propose a new Self-adaptive Collective Intelligence (CI) Differential Evolution algorithm with a restart mechanism (SaCIDE-*r*) for optimizing the economic scheduling of a shipboard microgrid.

CI [53] is defined as a type of group intelligence derived from collective efforts, the collaboration, and competition of many members and appears in consensus decision-making. Usually, the decision made by a group is often better than the decision made by a single individual. CI can be defined as a process of collecting opinions or information of the individuals in a group, and then constructing the information to make a more promising decision. This new intelligence can be formed in humans and computer networks, animals, bacteria, and appears in many forms of consensus decision-making mode. It has been widely used in various engineering problems, such as forecast [54], wireless sensor network [55], business [56], nonlinear optimization [57], max power point tracking [58], and debugging [59]. Thus, we are trying to combine this technique with DE algorithm to find better solutions of the economic scheduling of a shipboard microgrid.

This paper aims at optimizing economic day-ahead dispatch of a shipboard microgrid. Such a control model usually provides a series of outputs of DG and the battery system 24 hours ahead. For land-based large-scale microgrids, history data of WT, PV and loads are easily stored, as a result, total annual cost is widely used. Whereas, for shipboard microgrids, data of renewable sources change frequently among different shipping lines. It is difficult to store the data and evaluate the cost annually. Thus, a day-ahead scheduling in 24 hours is the most widely used mode, which is different from some researches on optimizing economic dispatch of microgrids in seconds or minutes. Those investigations usually focus on the performances of controllers of DC/AC inverters. This paper presents an improved DE algorithm named as SaCIDE-*r* combined with CI and a restart mechanism. The main features are summarized as follows:

- We propose a new CI-based mutation operator which mixes the potential valuable information of  $m$  best vectors. Furthermore, the  $m$  value is self-adapted by a new presented exponential function.
- A re-initialization strategy is introduced when the population meets a stagnation.

The rest of paper is organized as follows. Section 2 describes the basic framework of a shipboard microgrid and models of power sources. Section 3 provides the math model of the multi-objective optimization problem of economic

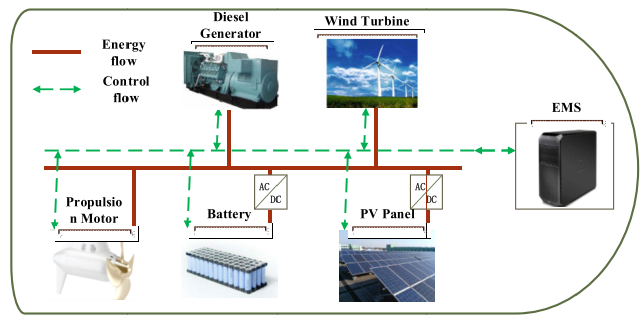


**FIGURE 1.** The structure of the shipboard microgrid.

scheduling for a shipboard microgrid. Section 4 presents the structure of the proposed SaCIDE-*r* algorithm and numerical experiments on CEC 2013 test functions. Section 5 describes the implement of this proposed method to optimizing the scheduling of a shipboard microgrid. Section 6 conducts case studies with different scenarios compared with other multi-objective algorithms. Finally, this paper is concluded in Section 7.

## II. FRAMEWORK OF SHIPBOARD MICROGRID

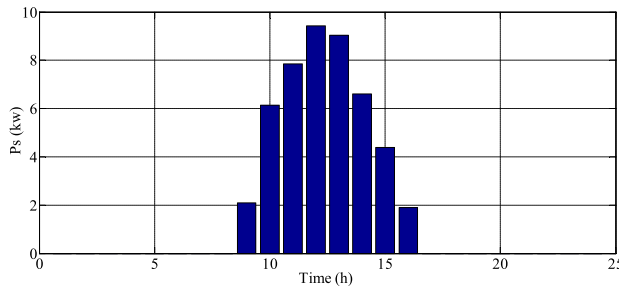
### A. STRUCTURE OF SHIPBOARD HYBRID MICROGRID

First of all, we should give a description of the basic structure of a shipboard microgrid mixed with some types of power sources. As shown in Fig. 1, the shipboard microgrid consists of DG, PV, WT, battery system and loads. These components are controlled by an EMS and connected through power lines (red) and communication lines (green). Among the power sources there are two types: non-dispatchable sources (PV, WT) and dispatchable sources (DG, battery). In this paper, it is assumed that the EMS controls the operations of the shipboard microgrid. In most cases, shipboard microgrids operate in an islanded mode. It should be noticed that this paper uses a day-ahead control mode which calculates outputs of the controllable power sources at each hour in a day. First, the EMS will forecast the output power of PV, WT and loads required in the next day. Second, based on these information and the State of Charge (SOC) of the battery system, the outputs of all dispatchable sources are calculated to obtain the total losses of the shipboard microgrid. Generally speaking, the charging and discharging losses of the battery system and the fuel costs must be considered. Differential from other terrestrial microgrids, shipboard microgrid barely operates in the grid-connected mode. Thus, we do not concern the electricity price. In the following parts, we will introduce the math models of power sources on board.

### B. SOLAR GENERATOR MODEL

Considering the size and the efficiency of PV generator, it could be determined as a function as follows [30]:

$$P_s = \eta_s \cdot A \cdot SI (1 + \gamma (t_0 - 25)) \quad (1)$$

**FIGURE 2.** Predicted output powers of PV in 24 hours.

where  $\eta_s$  is the efficiency of PV generators;  $A$  is the area of PV panels;  $SI$  represents the solar irradiation;  $t_0$  is the air temperature;  $\gamma$  is the temperature coefficient of the maximum output power. Usually, the power outputs of PV in the next day are forecasted based on the history data. To make our investigation focused, it is assumed that the outputs are already calculated. Fig. 2. Shows an example of predicted output power of a PV generator over a 24 h horizon.

### C. WIND TURBINE MODEL

The output power of a WT relies on wind velocities at the turbine power rating and wind speed. The function of output power could be built up as follows [60]:

$$P_w = \begin{cases} 0 & \text{if } v \geq v_f \mid v \leq v_c \\ P_r \frac{v^3 - v_c^3}{v_r^3 - v_c^3} & \text{else if } v_c < v < v_r \\ P_r & \text{otherwise} \end{cases} \quad (2)$$

where  $v$  refers to the wind speed;  $v_c$  and  $v_f$  denote the cut-in and the cut-off wind speed, respectively;  $v_r$  is the rated wind speed;  $P_r$  represents the rated electrical power of WT. Similar with the output power of PV, in this study, the outputs of WT day-ahead are already forecasted and stored in the EMS. Fig. 3 provides the predicted outputs over a 24 h horizon.

### D. BATTERY SYSTEM MODEL

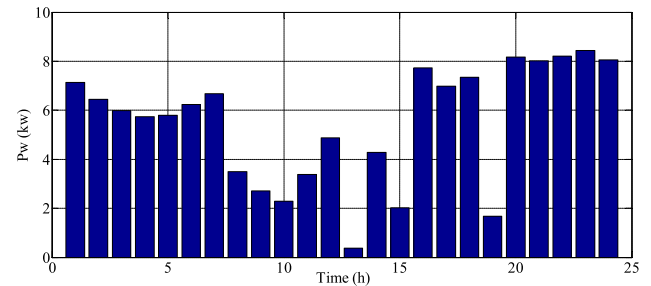
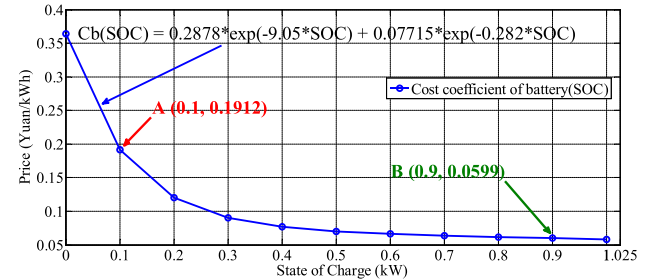
In this paper, we choose lithium-ion (Li-ion) batteries as the storage system instead of flywheel, fuel cell and superconducting magnetic energy storage. Li battery is one of the most popular storage systems and widely used in terrestrial microgrid due to the higher ratio of energy over weight and a slow loss of charge during idle conditions [61]. The charging-discharging performance of the battery is described with respect to SOC as follows [30]:

$$SOC(T) = SOC(T - 1) + \Delta T P_c(T) \eta_c \quad (3)$$

$$SOC(T) = SOC(T - 1) - \Delta T P_d(T) / \eta_d \quad (4)$$

where  $\eta_d$  and  $\eta_c$  are the discharging and charging efficiencies, respectively;  $\Delta t$  is the interval of the simulation period and set to 1 hour in this study;  $P_c(t)$  is the charging power at  $t$ th time;  $P_d(t)$  is the discharging power at  $t$ th time.

Power exchanges between the battery and a hybrid microgrid will lead to frequent charging/discharging processes of

**FIGURE 3.** Predicted output powers of WT in 24 hours.**FIGURE 4.** The cost characteristics of a battery system with respect to SOC.

the battery system. It is generally accepted that, the battery system has a larger capital investment and shorter lifetime than the other devices in the microgrid. Thus, it is not a negligible cost which is associated with the degradation of the battery system. Usually, the loss cost per kWh of a battery system is a function of SOC [28]. Fig. 4 illustrates the relationship between the cost coefficient and SOC. In that figure, point A denotes that the loss cost of the battery system is 0.1912 ¥/kWh with SOC is 0.1. Point B represents the loss cost of the battery system is 0.0599 ¥/kWh when SOC is 0.9.

## III. MATH MODEL OF THE OPTIMIZATION PROBLEM

In this part, we would like to give the math model of the multi-objective optimization, *i.e.*, economic scheduling of a shipboard microgrid. There are two non-compatible objectives or criteria, which are minimizing the fuel consumption and the cycle degradation of the battery system. A series of feasible solution points, which are call Pareto front, should be found to meet the economic goal. Next, the objective functions will be built up as follows.

### A. OBJECTIVE FUNCTIONS

First of all, the primary concerning of a shipboard microgrid is to reduce the fuel cost. It is noticed that the problem is investigated in a 24-hours period. Therefore, a day time intervals with different load demands are considered in the calculation. The total cost consists of the fuel cost is formulated in the below.

$$f_1 = \min \sum_{t=1}^T \sum_{i=1}^{N_{DG}} (C_F + C_E) P_{DG,i}(t) \quad (5)$$

where  $C_F$  and  $C_E$  are the cost coefficients of fuel consumption and emission for the DGs, respectively;  $P_{DG,i}$  denotes the output power of the  $i$ th DG;  $N_{DG}$  is the total number of generators on board.

For a shipboard microgrid, to reduce the total life losses of the battery system is also very important. In this paper, an objective function which considers degradation cost of charging-discharging cycles of a battery system is proposed as follows [30]:

$$f_2 = \min \sum_{t=1}^T \sum_{j=1}^{N_B} C_B |P_{B,j}(t)| \quad (6)$$

where  $C_B$  denotes the cost coefficient of the battery system;  $P_{B,j}$  represents the output power of the  $j$ th battery;  $N_B$  is the total number of batteries on board.

From the above objectives we can see, in this study, the optimization problem consists of two objectives which are not compatible to each other. The requirement from load at time  $t$  must be satisfied on board. If output power of the battery system is high, then the output power of DG will be low, resulting in a big fitness value of  $f_1$  and a small fitness value of  $f_2$ , and vice versa. These two objectives could not be satisfied at the same time.

## B. CONSTRAINTS

The objective functions should be subjected to the following constraints:

$$P_{DG}^{\min} \leq P_{DG}(t) \leq P_{DG}^{\max} \quad (7)$$

$$P_B^{\min} \leq P_B(t) \leq P_B^{\max} \quad (8)$$

$$SOC_{\min} \leq SOC(t) \leq SOC_{\max} \quad (9)$$

$$P_{PV}(t) + P_{WT}(t) + P_{DG}(t) + P_B(t) = P_L(t) \quad (10)$$

where  $P_L(t)$  means the demand of loads;  $P_{DG}^{\min}$  and  $P_{DG}^{\max}$  denote the lower and upper limits of output power for DG at time  $t$ , respectively;  $P_B^{\min}$  and  $P_B^{\max}$  denote the lower and upper limits of output power for the battery at time  $t$ , respectively.

A multi-objective optimization (MOP) problem [62] is defined as an optimization problem with more than one conflict meaning targets. As we have mentioned before, each objective is not compatible to the others. Thus, a series of solutions which are named as Pareto front should be resulted. The general formulation of an MOP with constraints could be described as follows:

$$\begin{aligned} \min F(\mathbf{X}) &= \{f_1(\mathbf{X}), f_2(\mathbf{X}), \dots, f_N(\mathbf{X})\} \\ \text{subject to : } &\begin{cases} g_i(\mathbf{X}) = 0 & i = 1, 2, \dots, m \\ h_j(\mathbf{X}) \leq 0 & j = 1, 2, \dots, n \end{cases} \quad (11) \end{aligned}$$

where  $F(\mathbf{X})$  denotes the objective functions;  $\mathbf{X}$  is the vector of the control variables;  $g_i(\mathbf{X})$  and  $h_j(\mathbf{X})$  represent the constraints of equality and inequality, respectively. It is assumed that,  $\mathbf{X}_1$  and  $\mathbf{X}_2$  are two optimized solutions for a MOP. The nomination solution which means that if and only if  $\mathbf{X}_1$

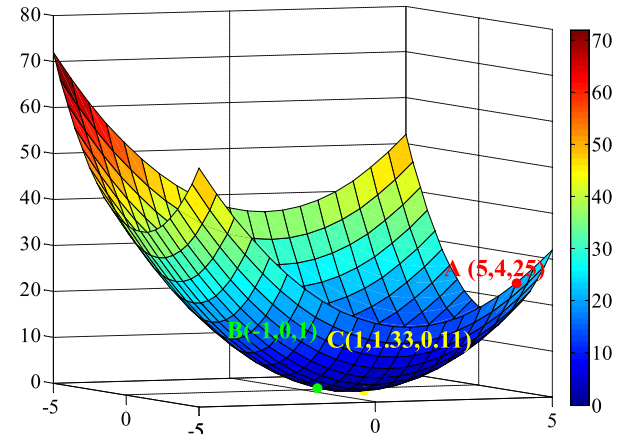


**FIGURE 5.** Illustration of a CI-based solution through a simple minimization function.

partially less than  $\mathbf{X}_2$  is formulated as below:

$$\begin{cases} f_i(\mathbf{X}_1) \leq f_i(\mathbf{X}_2), & \forall i = 1, 2, \dots, N \\ f_i(\mathbf{X}_1) \leq f_i(\mathbf{X}_2), & \exists i \in \{1, 2, \dots, N\} \end{cases} \quad (12)$$

Then we call that  $\mathbf{X}_1$  dominates  $\mathbf{X}_2$ . In the search space, the non-dominated solutions are considered as Pareto solutions. The Pareto front consists of non-dominated solutions.

For the above multi-objective economic scheduling problem of a shipboard hybrid microgrid, it is necessary to develop a powerful algorithm to find the optimal and feasible solutions. The optimization problem in this paper is a MOP with some equality and inequality constraints. In the next part, we will give a full descriptions on the proposed SaCIDE-*r* algorithm for solving this problem.

## IV. SaCIDE-R ALGORITHM

In this section, we would like to present all the evolutionary operators with a restart mechanism and the adaptions of control parameters of the presented SaCIDE-*r* algorithm.

### A. MOTIVATION OF CI-BASED MUTATION

For most DE variants, the mutant vectors are composed of either randomly selected vector or/and the best vector in the current population. Here, we are trying to show the motivation of using CI-based mutation strategy to improve the performance of a DE algorithm. A simple illustration is given below.

It is considered that there is a very simple minimizing optimization function with two variables. The function is shown as follows:

$$f(x) = (x_1 - 1)^2 + (x_2 - 1)^2, \quad x_i \in [-5, 5] \quad (13)$$

Meanwhile, a 3D fitness landscape of this function is plotted shown as Fig. 5.

In the above figure, there are two solutions A (5, 4) which is marked as red color and B (-1, 0) which is marked as green color. In current population, the rank of fitness value  $r_A$  is 8, and the rank of fitness value  $r_B$  is 4. By using a CI-based linear combination, the new solution C (1, 1.33) with a fitness

value 0.11 could be calculated as follows:

$$C = \frac{r_B}{r_A + r_B} A + \frac{r_A}{r_A + r_B} B \quad (14)$$

After calculating the collective information of A and B, a new solution C with better fitness value is obtained. Thus, the CI-based calculation may provide a promising evolving direction to improve the searching efficiency. Although such an improvement is obtained by using a unimodal function, based on our previous experiments, it is also possible for multi-modal and composition functions. Thus, we would like to incorporate this CI-based theory into DE algorithm to generate more promising mutant vectors, resulting in more powerful exploration and exploitation capabilities.

### B. EVOLUTIONARY OPERATIONS OF SaCIDE-R

At each generation  $G$ , DE algorithm evolves a population, which could be presented as  $\mathbf{X}_{i,G} = (x_{i,G}^1, x_{i,G}^2, \dots, x_{i,G}^D | i = 1, 2, \dots, NP)$ , where  $NP$  is the population size,  $D$  is the dimension of the problem. After initialization the population is randomly generated within the search domains. Conventional DE algorithm is executed by the following three steps: mutation, crossover and selection.

This new mutation operator mixes collective information of some top ranked and randomly selection vectors to generate mutant vector as follows:

$$\begin{aligned} \mathbf{V}_{saci\_i,G} &= \mathbf{X}_{i,G} + F \cdot (\mathbf{X}_{saci\_best,G} - \mathbf{X}_{i,G}) + F \cdot (\mathbf{X}_{r_1^i,G} - \mathbf{X}_{r_2^i,G}) \\ &= \mathbf{X}_{i,G} + F \cdot (\mathbf{X}_{saci\_best,G} - \mathbf{X}_{i,G}) + F \cdot (\mathbf{X}_{r_1^i,G} - \mathbf{X}_{r_2^i,G}) \end{aligned} \quad (15)$$

where  $\mathbf{X}_{saci\_best,G}$  is a composite vector mixed with some top ranked vectors at the  $G$ th generation.  $\mathbf{X}_{saci\_best,G}$  is denoted as follows:

$$\mathbf{X}_{saci\_best,G} = \sum_{k=1}^m w_k \cdot \mathbf{X}_{k,G} \quad (16)$$

where  $m$  denotes the number of top ranked vectors in the current population,  $w_k$  represents the weight of the  $k$ th selected vector  $\mathbf{X}_{k,G}$  within the group of  $m$  top ranked vectors at  $G$ th generation. In this paper, the weight for each selected vector is calculated as follows:

$$w_k = \frac{m - k + 1}{1 + 2 + \dots + m} \quad \text{for } k = 1, 2, \dots, m. \quad (17)$$

From the above equations we can see, the proposed mutation vector is a mixture of a linear combination of  $m$  top ranked vectors and two other randomly selected vectors. Different from DE/rand/1, such a mutation operator combines the information which come from some promising vectors with better fitness values in the current population based on CI theory, resulting in a better mutation vector. As we mentioned before, the decision made by a single individual is usually worse than the decision made by a group. Thus, the proposed CI mutation operator may guide the donor vector towards potential better searching areas compared with DE/rand/1 and other mutation strategies. In this

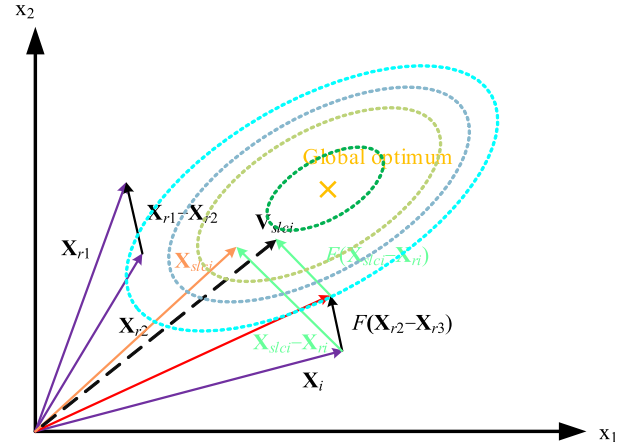


**FIGURE 6. Illustrating mutation scheme of proposed CI-based mutation operator in 2D parametric space.**

paper, the whole self-adaption of  $m$  could be described as follows [63]: (1) generate the probability  $p_i$  of exponentially distributed random number whose mean is  $\mu$  for each target vector  $i$ ; (2) generate  $m_i$  for  $i$ th target vector according to  $p_i$  by using roulette wheel selection; (3) if a better trial vector is obtained, the  $m_i$  value would be added into the successful record which is named as  $S_m$ ; (4) estimate the mean value  $\mu$  of the successful record  $S_m$ ; (5) go to step (1). The process of CI-based mutation strategy on a 2D parameter space is shown Fig. 6. In the following figure, a better mutation vector is generated by using the proposed CI-based mutation strategy obviously.

In the conventional version, the binomial crossover operator is often used as follows [34]:

$$u_{saci,G}^j = \begin{cases} v_{saci,G}^j, & \text{if } rand_j \leq Cr \text{ or } j = j_{rand} \\ x_{i,G}^j, & \text{otherwise} \end{cases} \quad j = 1, 2, \dots, D \quad (18)$$

where the control parameter of crossover rate  $Cr$  is a positive value within  $[0, 1]$ ,  $j_{rand}$  is an integer randomized within  $[1, D]$ ,  $rand_j$  is a random number obeys uniform distribution generated within  $[0, 1]$  at  $j$ th dimension.

The selection operator is usually defined as follows:

$$\mathbf{X}_{i,G+1} = \begin{cases} \mathbf{U}_{saci,G}, & \text{if } f(\mathbf{U}_{saci,G}) < f(\mathbf{X}_{i,G}) \\ \mathbf{X}_{i,G}, & \text{otherwise} \end{cases} \quad (19)$$

For adapting control parameters of SaCIDE, leaving  $NP$  as a fixed value, we adapt  $F$  and  $Cr$  in a relatively simple but effective manner. The equations are shown as follows [64]:

$$F_{i,G+1} = \begin{cases} F_l + r_1 \cdot F_u, & \text{if } r_2 < \tau_1 \\ F_{i,G} & \text{otherwise} \end{cases} \quad (20)$$

$$Cr_{i,G+1} = \begin{cases} r_3, & \text{if } r_4 < \tau_2 \\ Cr_{i,G} & \text{otherwise} \end{cases} \quad (21)$$

where  $r_1, r_2, r_3, r_4$  are uniform random values within  $[0, 1]$ ,  $\tau_1$  and  $\tau_2$  are two positive values to adjust  $F$  and  $Cr$  both setting to 0.1 in our experiments,  $F_l$  is the lower limit of  $F$  set to 0.1,  $F_u$  is the upper limit of  $F$  set to 0.9.

In summary, the pseudo code of the proposed SaCIDE algorithm is described as Algorithm 1.

#### Algorithm 1 The Main Structure of SaCIDE

Initialize and evaluate  $\mathbf{X}$

**While**  $G \leq G_{max}$  **DO**

**For**  $i = 1: NP$

$$\begin{aligned} \mathbf{V}_{saci\_i,G} &= \mathbf{X}_{i,G} + F_i \cdot (\mathbf{X}_{saci\_best,G} - \mathbf{X}_{i,G}) \\ &\quad + F_i \cdot (\mathbf{X}_{r_1^i,G} - \mathbf{X}_{r_2^i,G}); \end{aligned}$$

**For**  $j = 1: D$

**If**  $U(0,1) \leq Cr_i$ ,  $u_i^j = v_{saci}^j$

**Else**  $u_i^j = x_{saci}^j$

**End**

**If**  $f(\mathbf{U}_i) \leq f(\mathbf{X}_i)$ ,  $\mathbf{X}_i = \mathbf{U}_i$

**Renew**  $F_i, Cr_i$

**End**

**End**

#### C. RE-INITIALIZATION

From our previous experimental results, the current version of SaCIDE still suffers from a premature and a stagnation, although the performances on benchmark functions have been improved to some extent. Generally speaking, premature convergence occurs when the population is trapped in local optima. If the population will not find any better solutions although the whole population is diversified, then such a condition is called stagnation. It is very effective to re-initialize the population for dealing with a premature convergence and a stagnation. Both of the above two circumstances could be detected by using the following equation:

$$stg_{G+1} = \begin{cases} 0 & f(\mathbf{U}_i) < f(\mathbf{X}_i) \forall i \in \{1, 2, \dots, NP\} \\ stg_G + 1 & f(\mathbf{U}_i) \geq f(\mathbf{X}_i) \exists i \in \{1, 2, \dots, NP\} \end{cases} \quad (22)$$

where  $stg_G$  is an indicator which is used to monitor if the current population meets a stagnation at  $G$ th generation. If any trial vector has a better fitness value than the corresponding donor vector, then it means the population is not stagnant at all. On the contrary, if all the trial vectors in the population have worse fitness values than the donor vectors, the indicator  $stg_G$  would be added by 1. When  $stg_G$  reaches to a threshold value  $stg_{max}$ , resulting in a stagnant population, the restart mechanism is triggered. In this study, the whole population is re-initialized within the searching ranges but remaining the  $m$  top ranked individuals. Such a design is to make a trade-off between a diversified population with no searching directions and currently promising searching directions. Adopting similar presentation in [65], by incorporating this

**TABLE 1. Parameter settings of involved DE algorithms.**

Methods	Parameters settings
SaDE [67]	$F = \text{Norm}(0.5, 0.3)$ , $Cr = \text{Norm}(Cr_{mk}, 0.1)$ , $LP = 50$
JADE [68]	$c = 0.1$ , $p = 0.05$ , $\mu_F = 0.5$ , $\mu_{CR} = 0.5$
jDE [65]	$F_l = 0.1$ , $F_u = 0.9$ , $\tau_1 = \tau_2 = 0.1$
AS-JADE [69]	$c = 0.1$ , $p = 0.05$ , $\mu_F = 0.5$ , $\mu_{CR} = 0.5$ , $\alpha = 0.3$ , $\beta = 0.8$
CoDE [38]	$F_1 = 1$ , $Cr_1 = 0.1$ , $F_2 = 1$ , $Cr_1 = 0.9$ , $F_3 = 0.8$ , $Cr_3 = 0.2$
rank-jDE [41]	$F_l = 0.1$ , $F_u = 0.9$ , $\tau_1 = \tau_2 = 0.1$
CIMDE/rand/1 [53]	$F = 0.5$ , $Cr = 0.9$
SaCIDE-r	$F_l = 0.1$ , $F_u = 0.9$ , $\tau_1 = \tau_2 = 0.1$ , $stg_{max} = 100$

re-initialization scheme, the whole SaCIDE-r algorithm is described as Fig. 7.

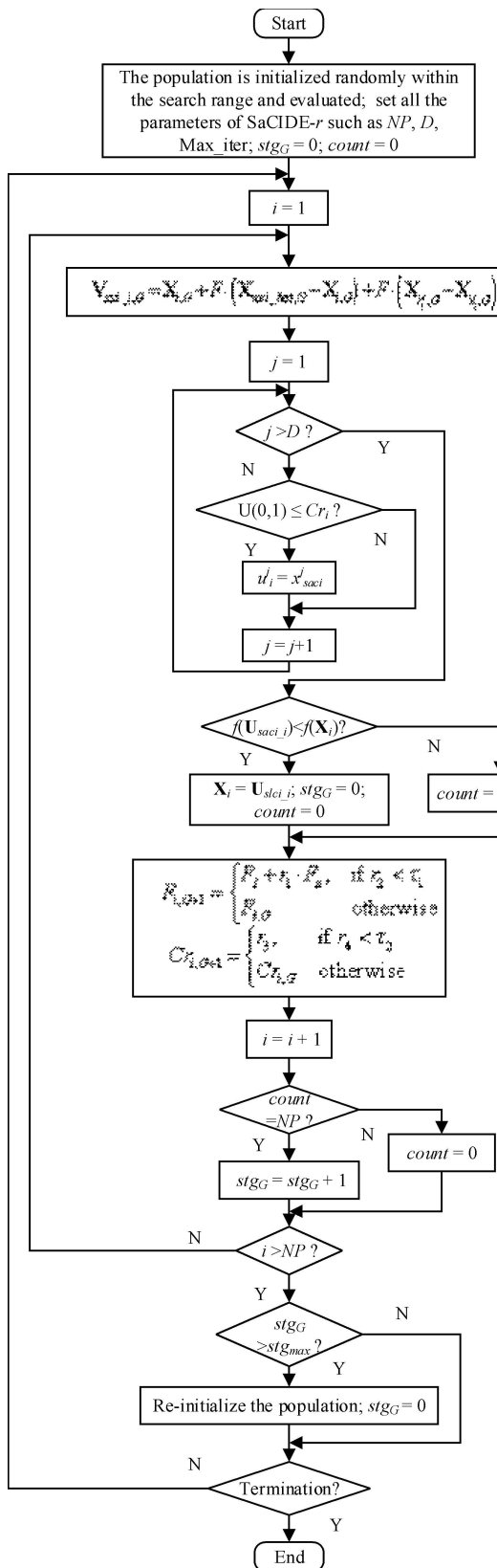
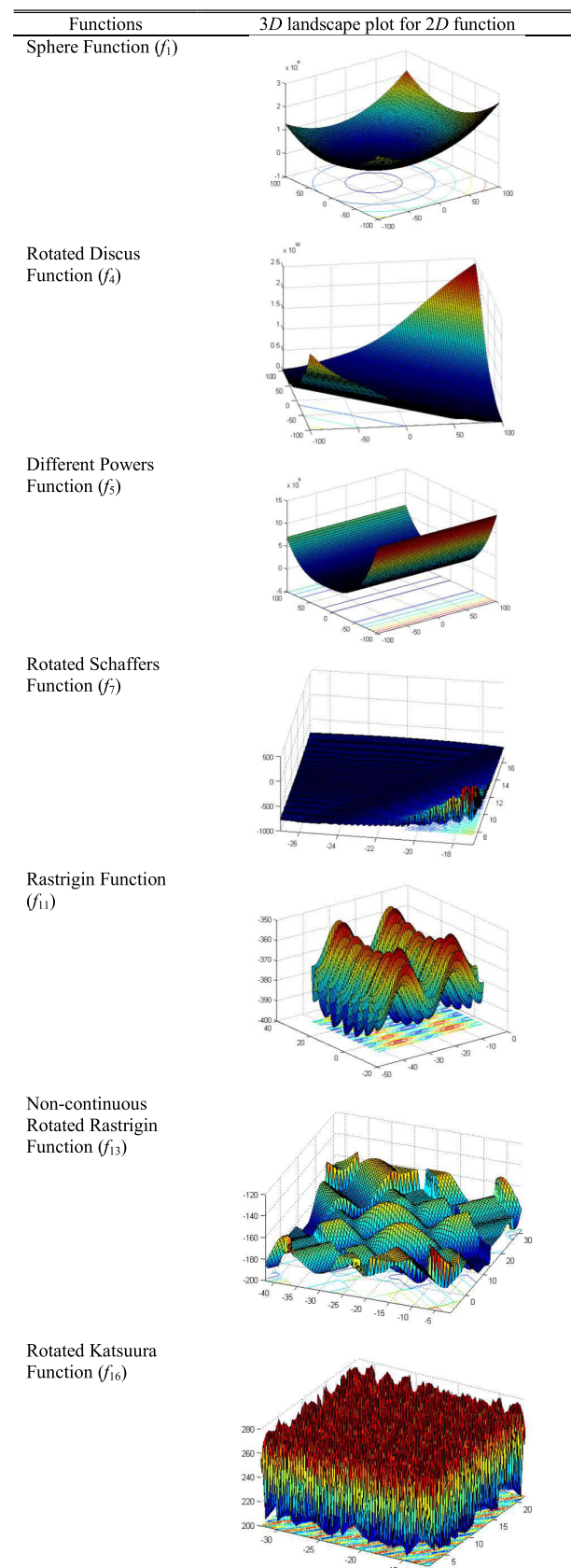
#### D. EXPERIMENTAL RESULTS ON CEC2013 FUNCTIONS

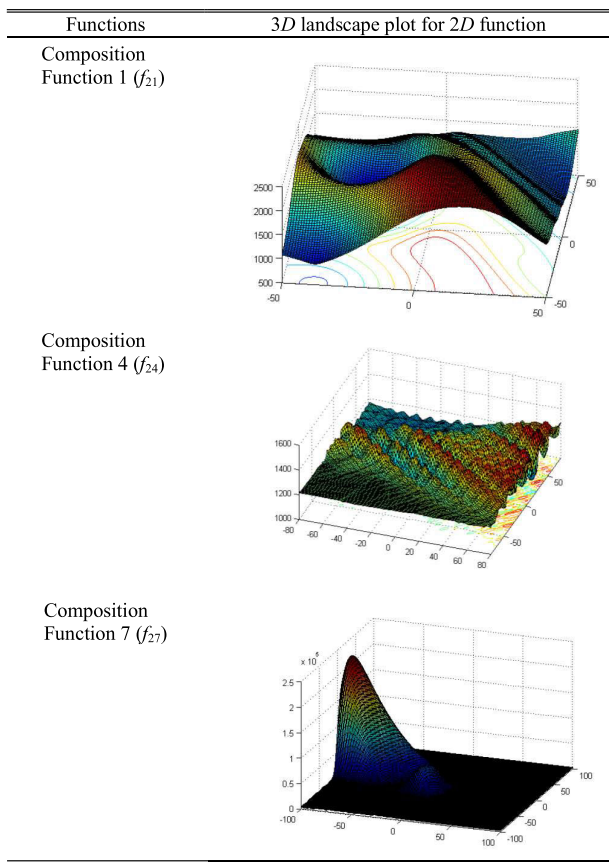
In this part, we would like to conduct comprehensive experiments to prove the effectiveness of the proposed SaCIDE-r algorithm, compared with seven other state-of-the-art DE algorithms. First, to test the performance on global optimization problems, we select ten CEC2013 benchmark functions with distinctive fitness landscapes with  $D = 30$ . The overall accuracies and convergence curves will be reported. In this paper, we adopted a Windows 10 operating system and the MATLAB 2018a development environment as the simulation platform. For fair comparisons, we chose the following seven state-of-the-art DE algorithms shown in Tab. 1 with their recommended setups.

The descriptions of the chosen functions are shown in Tab. 2. According to the properties, these test functions are classified into three types: uni-modal problems ( $f_1, f_4, f_5$ ), basic multi-modal problems ( $f_7, f_{11}, f_{13}, f_{16}$ ) and composition problems ( $f_{21}, f_{24}, f_{27}$ ).

For all the test functions and the algorithms, NP was set to 100. The max Function Evaluations (Max\_FEs) was set to 10000D. All the different algorithms on each benchmark function were conducted over 31 independent runs. The error values of all DE variants were given in Tab. 3 with  $D = 30$ . To show the significance between the presented method and another competitor, we also conducted the Wilcoxon rank sum test at 0.05 level [69], [70], regarding SaCIDE-r vs. another one as “+”, “-”, “≈”. “+” (win) means the proposed method is significantly better than another algorithm, “-” (lose) represents the proposed method is significantly worse than another algorithm, and “≈” (tie) denotes the proposed method is significantly equal to another algorithm. The comparison results were summarized as “w/t/l” in the following tables. The best results among the comparison were shown in bold.

From Tab. 3 we can see, the proposed method has beaten the other algorithms on 3 to 7 test functions. Meanwhile, SaCIDE-r algorithm was only defeated by SaDE on  $f_{11}$ , rank\_jDE on  $f_1$  and  $f_4$ . Take JADE as an example, SaCIDE-r algorithm has outperformed JADE on 5 test functions ( $f_4, f_7, f_{11}, f_{13}, f_{16}$ ). SaCIDE-r algorithm was not defeated on any test functions. On the rest 5 test functions,

**TABLE 2.** Summary of the selected 10 CEC2013 test functions.**FIGURE 7.** The technical strategy block diagram of the proposed method.

**TABLE 2.** (Continued.) Summary of the selected 10 CEC2013 test functions.

there was no significant difference between the presented method and JADE. In general, the proposed method may have a more powerful global searching capability compared with some state-of-the-art DE algorithms on some benchmark functions. Next, all the median convergence curves of the compared algorithms on the test functions are plotted in Fig. 8.

## V. APPLICATION FOR SCHEDULING SHIPBOARD MICROGRID USING SaCIDE-R

In this section, the authors would like to give the steps of applying the proposed SaCIDE-*r* algorithm for economic scheduling of a shipboard microgrid. As mentioned above, it is noticed that this investigation focuses on a day-ahead economic scheduling with two objectives on board. Before running the optimizing program in the EMS, the output power of WT, PV and load are forecasted by other algorithms. Assume that there is no uncertainties between the forecasted power and the real power. In order to minimize the costs of fuel consumption and the battery system, the power generation from WT and PV should be used preferentially to meet the demand of loads at any time. If the sustainable power is not high enough for the load demand, then the rest required power should be supplied by the battery system or the DG.

To make the optimization problem easy to solve, a single solution is defined as follows:

$$\mathbf{X} = [P_{B1}, P_{B2}, \dots, P_{Bt}, \dots, P_B] \quad (23)$$

$$P_{Bi} = \begin{cases} P_d & \text{if } P_{Bi} > 0 \\ P_c & \text{otherwise} \end{cases} \quad (24)$$

In this paper, it means the battery system is discharging when  $P_{Bi}$  is a positive value, and it denotes that the battery system is charging when  $P_{Bi}$  is a negative value. A time  $t$ , the searching range and initializing range of  $\mathbf{X}$  should be restricted within  $[-P_B^{\max}, P_L(t) - P_{PV}(t) - P_{WT}(t)]$ . Then the rest power should be balanced by adjusting the output power of the DG. Such a solution  $\mathbf{X}$  will be evaluated to calculate the fitness values. The steps of applying SaCIDE-*r* for multi-objective economic scheduling of a shipboard microgrid are listed as follows:

*Step 1:* Load the power of PV, WT and required loads in the next 24 hours.

*Step 2:* Set the parameters of the simulation, such as  $NP$ ,  $Max\_FEs$ , independent run times and simulation scenarios.

*Step 3:* The population is initialized within the searching ranges and evaluated. Each vector should be evaluated for each objective according to Eq. (5-6).

*Step 4:* For each donor vector, the mutation operation is conducted according to Eq. (15).

*Step 5:* For each mutant vector, the crossover operation is conducted according to Eq. (18).

*Step 6:* For each trial vector, the variable should be restricted within the searching domain at each dimension.

*Step 7:* For each trial vector, two fitness values of the two objectives should be calculate. The donor vector is replaced by the generated trial vector when both the two fitness values are better. Otherwise,  $stg_G$  is added by 1.

*Step 8:* The control parameters of the proposed method should be adapted according to Eq. (20-21).

*Step 9:* If  $stg_G$  is bigger than  $stg_{\max}$ , then the reinitialization is triggered; otherwise, go to the next step.

*Step 10:* If the termination criteria are met, then output the best solution and plot the Pareto front; otherwise, go to Step 4.

To show how to apply SaCIDE-*r* for shipboard microgrids and other large scale microgrids, the block diagram is given below:

## VI. CASE STUDIES

In this paper, the presented SaCIDE-*r* is applied for multi-objective economic scheduling of a shipboard microgrid. For a specific ship, there are two typical working conditions which are the harbor mode and the voyage mode. In the harbor mode, load demand changes frequently and dramatically. Whereas, in the voyage the load demand barely changes. All the simulations are run under islanded mode. The parameters of the involved shipboard microgrid are shown in Tab. 4 and 5. The capacity settings come from a hybrid microgrid in a

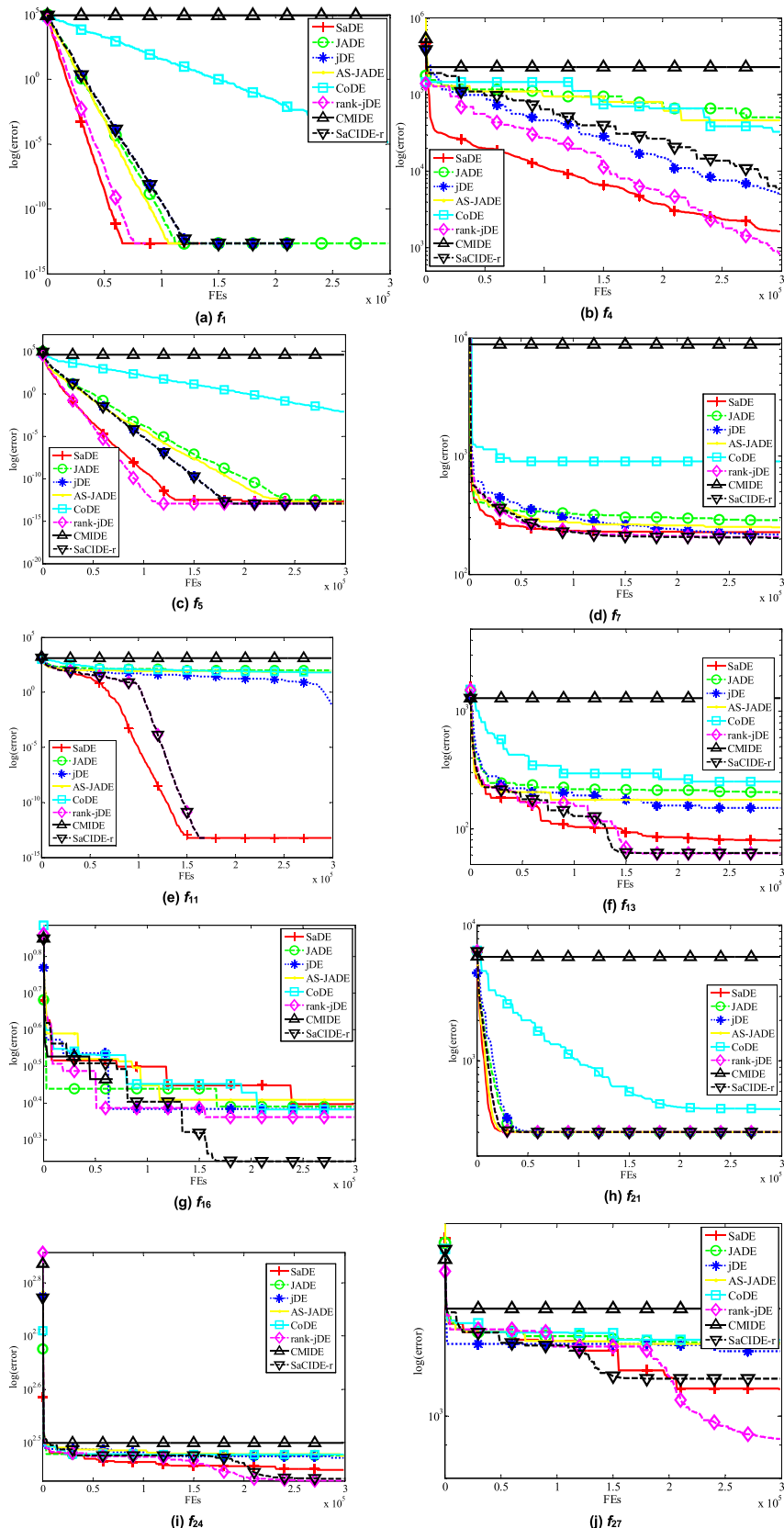


**FIGURE 8.** The median convergence curves of the involved algorithms on CEC test functions with  $D = 30$ .

**TABLE 3.** Compared results of competitors and SLCIDE algorithm on test functions with D = 30.

No.	SaDE	JADE	jDE	AS-JADE
$f_1$	7.33E-14±1.08E-13 (≈)	2.27E-13±0.00E+00 (≈)	7.33E-15±4.08E-14 (≈)	2.93E-14±7.75E-14 (≈)
$f_4$	1.58E+03±9.21E+02 (≈)	5.33E+04±1.50E+04 (+)	5.29E+03±1.77E+03 (≈)	4.74E+04±1.09E+04 (+)
$f_5$	1.76E-13±5.75E-14 (≈)	3.78E-13±1.03E-13 (≈)	<b>1.03E-13±3.42E-14</b> (≈)	1.50E-13±5.40E-14 (≈)
$f_7$	2.59E+01±1.35E+01 (+)	9.23E+01±3.27E+01 (+)	1.84E+01±1.29E+01 (+)	4.97E+01±2.01E+01 (+)
$f_{11}$	<b>7.33E-14±2.62E-14</b> (-)	9.90E+01±9.42E+00 (+)	1.17E+00±1.88E+00 (+)	6.81E+01±9.83E+00 (+)
$f_{13}$	7.98E+01±1.71E+01 (+)	2.08E+02±1.98E+01 (+)	1.52E+02±1.18E+01 (+)	1.77E+02±1.55E+01 (+)
$f_{16}$	2.45E+00±2.40E-01 (+)	2.48E+00±2.17E-01 (+)	2.45E+00±2.16E-01 (+)	2.55E+00±2.47E-01 (+)
$f_{21}$	3.12E+02±7.51E+01 (≈)	2.97E+02±9.56E+01 (≈)	2.77E+02±4.25E+01 (≈)	2.97E+02±7.81E+01 (+)
$f_{24}$	2.82E+02±6.18E+00 (≈)	2.99E+02±3.50E+00 (≈)	2.96E+02±2.67E+00 (≈)	2.99E+02±2.55E+00 (≈)
$f_{27}$	1.11E+03±1.11E+03 (≈)	1.30E+03±2.96E+01 (≈)	1.26E+03±2.41E+01 (≈)	1.28E+03±3.39E+01 (≈)
w/t/l	3/6/1	5/5/0	4/6/0	6/4/0
No.	CoDE	rank-jDE	CIMDE/rand/1	SaCIDE-r
$f_1$	1.37E-05±3.24E-06 (+)	<b>0.00E+00±0.00E+00</b> (-)	8.52E+04±1.15E+04 (+)	4.10E-11±5.77E-11
$f_4$	3.49E+04±1.54E+04 (+)	<b>9.16E+02±4.45E+02</b> (-)	2.51E+05±9.35E+04 (+)	2.14E+03±9.05E+02
$f_5$	7.51E-03±1.23E-03 (+)	<b>1.03E-13±3.42E-14</b> (≈)	4.07E+04±1.11E+04 (+)	1.76E-12±2.34E-12
$f_7$	6.92E+02±1.40E+02 (≈)	8.87E+00±6.13E+00 (≈)	4.48E+04±1.19E+05 (+)	<b>3.18E+00±5.49E+00</b> (+)
$f_{11}$	5.55E+01±4.59E+00 (+)	1.28E-01±3.39E-01 (+)	1.31E+03±1.51E+02 (+)	8.66E-05±9.71E-05
$f_{13}$	2.54E+02±1.10E+01 (+)	6.23E+01±1.42E+01 (+)	1.28E+03±1.53E+02 (+)	<b>9.88E+00±1.04E+01</b> (+)
$f_{16}$	2.37E+00±2.84E-01 (+)	2.15E+00±5.98E-01 (+)	<b>0.00E+00±0.00E+00</b> (-)	7.39E-04±6.11E-04
$f_{21}$	4.32E+02±4.76E+01 (≈)	2.84E+02±8.48E+01 (≈)	5.73E+03±6.87E+02 (+)	<b>2.17E+02±5.30E+01</b> (+)
$f_{24}$	3.01E+02±2.98E+00 (≈)	<b>2.67E+02±1.48E+01</b> (≈)	3.16E+02±3.92E+00 (≈)	2.69E+02±1.15E+01
$f_{27}$	1.31E+03±2.62E+01 (≈)	<b>9.23E+02±1.64E+02</b> (≈)	1.46E+03±4.49E+01 (≈)	1.08E+03±3.11E+01 (≈)
w/t/l	6/4/0	3/5/2	7/2/1	-

**TABLE 4.** Parameters of the renewable generators.

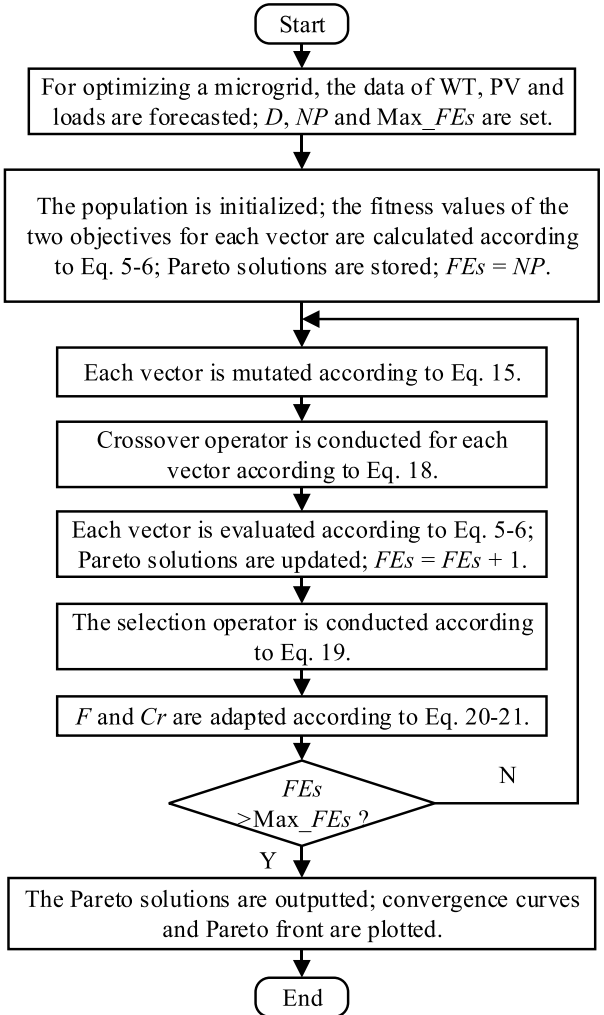
Type	$P_{max}$ (kW)	$P_{min}$ (kW)	$C_F$ (¥/kWh)	$C_E$ (¥/kWh)
PV	10	0	—	—
WT	10	0	—	—
DG	15	0	0.035	0.015

**TABLE 5.** Parameters of the battery system.

Parameters	Values
$P_{max,B}$ (kW)	4
$P_{min,B}$ (kW)	0
$C_B$ (¥/kWh)	$0.2878e^{-9.05SOC} + 0.07715e^{-0.282SOC}$
$E_{max}$ (kW)	40
$E_{min}$ (kW)	4
$SOC_{max} \cdot E_{max}$ per hour(kW)	5
$SOC_{min} \cdot E_{max}$ per hour(kW)	0
$SOC_0 \cdot E_{max}$ (kW)	28
$\eta_d$	0.9
$\eta_c$	0.9

barge, which mixes WT, PV, DG and the battery system to reduce the fuel cost and emissions.

The structure of the shipboard microgrid was displayed in Fig. 1. The math model of the objective functions and the corresponding constraints were given in Section II-III. For day-ahead economic scheduling of shipboard microgrid,

**FIGURE 9.** The block diagram of the proposed method.

$T$  is set to 24 in this study. For DE algorithms, there are three control parameters, which are  $F$ ,  $Cr$  and  $NP$ . For many DE variants,  $NP$  is usually fixed to a recommended value. In this paper,  $NP$  is set to 100 in numerical simulation and case studies. Such a setting is a widely used value.  $F$  and  $Cr$  are adapted according to Eq. 20-21. All the simulations are run in the same environment which was adopted in Section IV.

#### A. CASE 1: HARBOR MODE

In harbor mode, ships usually need frequent maneuverings, resulting in a frequent change of load. In this case, the forecasted power of WT, PV and load in 24 hours are plotted in Fig. 10.

For comparison, we conducted the simulation over 31 independent times by using four different algorithms, which are Multi-objective Differential Evolution (MODE) [71], Multi-objective Harmony Search (MOHS) [72], the well-known NSGA-II [73] and the proposed SaCIDE-r. For each independent run, the  $Max\_FEs$  is set to 10000. Some simulation results are shown in Fig. 11 to 13.

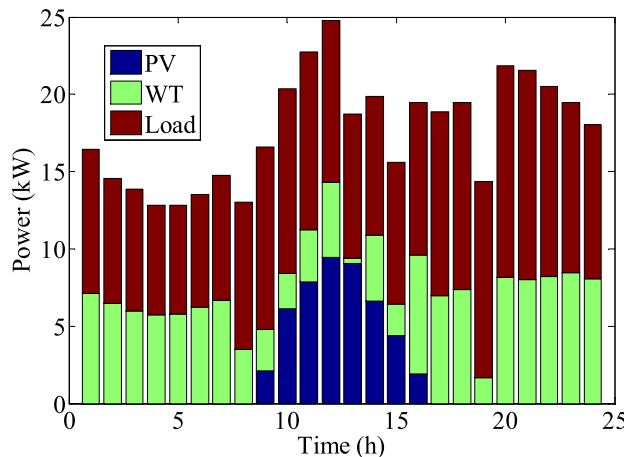


FIGURE 10. The forecasted power of PV, WT, and load in case 1.

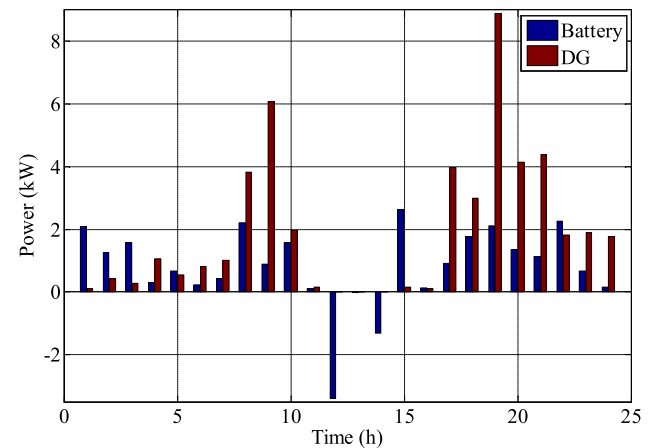


FIGURE 13. The generated power of the battery and DG by using SaCIDE-r for one run.

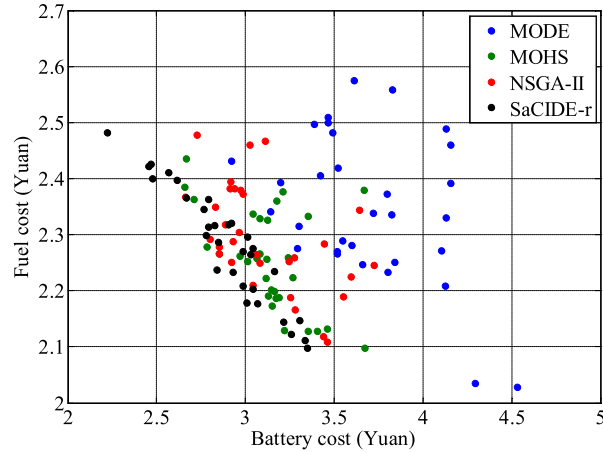


FIGURE 11. Comparison of the best solutions obtained by using different algorithms.

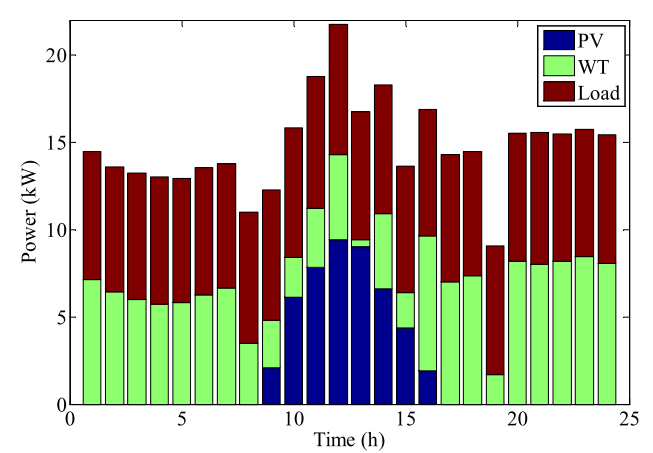


FIGURE 14. The forecasted power of PV, WT, and load in case 2.

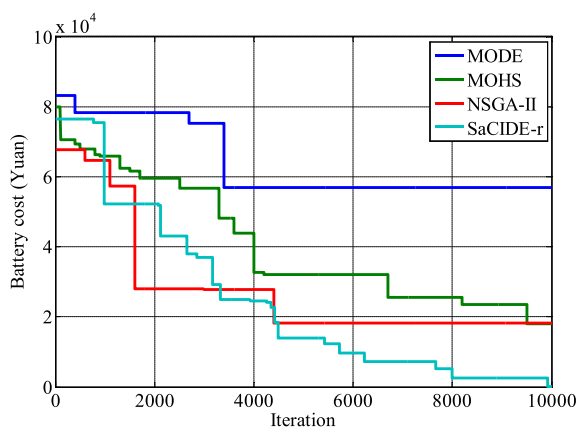
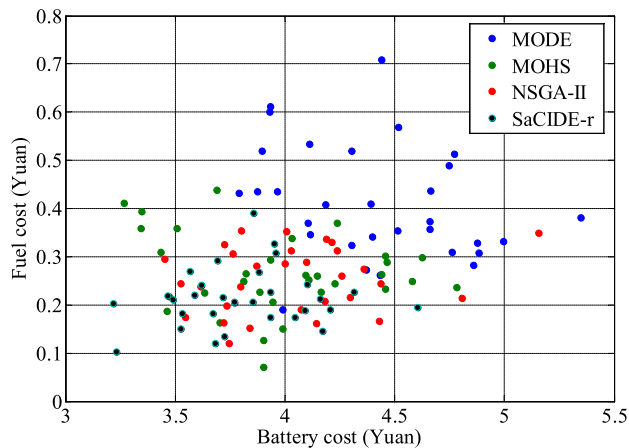


FIGURE 12. The median convergence curves of the involved algorithms for the objective of the battery cost.

All best solutions, which are found by using four algorithms run over 31 independent times, are plotted in the above figure. The spots marked with black color constituted a near-optimal Pareto front. Besides, the solutions found

by SaCIDE-r were more concentrated than other solutions. That means the proposed method has a more stable searching behavior. Compared with other algorithms, the proposed method is more suitable for this application.

It can be seen from Fig. 12 that the proposed algorithm has a more satisfying convergence curve than the other algorithms. During the evolution, the proposed method converged very fast. Besides, a sustainable searching behavior was displayed. When the iteration is bigger than 5000, none of the other algorithms could find better solution with smaller fitness value than SaCIDE-r. Fig. 13 shows the solution of the battery system and DG by using SaCIDE-r for a single run. It could be observed that in the time period  $t = 12 - 14$  h  $P_B(t)$  is negative and  $P_{DG}(t)$  is zero. At this time, the generation of PV and DG is more than the load demand, and the battery system is charging. Due to the relatively high and frequently changing load, the output power of DG is relatively high, resulting in a high fuel cost. Such a simulating result means that the supply power of DG is indispensable, especially when the renewable power sources could not afford the demand of loads in shipboard microgrids. From the above simulation



**FIGURE 15.** Comparison of the best solutions obtained by using different algorithms.

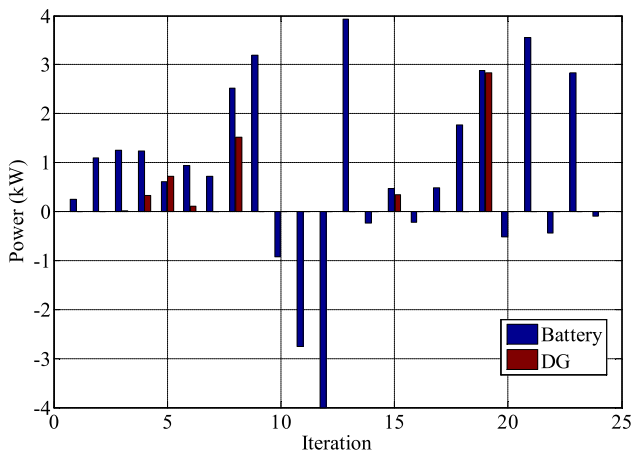


**FIGURE 17.** The generated power of the battery and DG by using SaCIDE-r for one run.

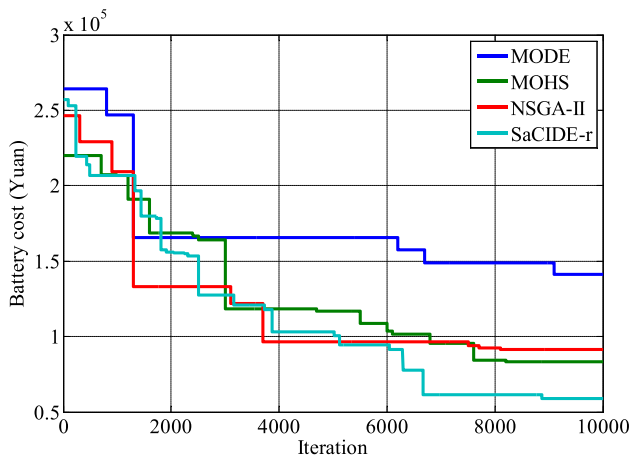


**FIGURE 16.** The median convergence curves of the involved algorithms for the objective of the battery cost.

results we can see, the proposed method has demonstrated the effectiveness for the multi-objective economic scheduling of a shipboard grid.

#### B. CASE 2: VOYAGE MODE

In voyage mode, the load demand of ships is usually fixed with a very small fluctuation. In this case, the forecasted power of WT, PV and load in 24 hours are plotted in Fig. 14. Also, the compared simulation results are shown in Fig. 15 to 16.

From the above figure, the performances of the four algorithms all deteriorated, resulting in a more scattered locations of the spots. In this case, the optimization problem seems harder than the former case, because the algorithms could not find the clear Pareto front. Nevertheless, the spots marked with black color still have better locations than other spots.

From the above figures we can see, the convergent performance of the proposed method is still better than the other algorithms. When the iteration is over 6000, none of the competitors has a better fitness value than the proposed method.

Compare with the first case, the fitness value of this case is bigger than the former, showing a more difficult optimization problem. Besides, due to the changes of the load demand, the output power of the battery and DG behave differently. In this simulation case, the sum of the generation power of PV and WT is often bigger than the load demand, resulting in more charging process for the battery system. And, the output power of DG has been much reduced compared with the first case, resulting in a much less fuel cost. It is also demonstrated that the total costs of shipboard microgrids rely on the demand of load and changes of the climate.

#### VII. CONCLUSION

With the growing demand for emission reductions and fuel efficiency improvements, alternative energy sources and energy storage technologies are becoming popular in ship microgrids. In order to balance the two non-compatible objectives, a new differential evolution variant was proposed to solve the optimization problem. In this algorithm, a CI-based mutation operator was proposed by mixing some promising donor vectors in the current population. Besides, a self-adaptive mechanism which was developed to avoid introducing extra control parameters. Further, to avoid being trapped in local optima, a re-initialization mechanism was developed. Then, we have evaluated the performances of the proposed SaCIDE-r approach by studying some numerical optimization problems of CEC 2013 with  $D = 30$ , compared with seven state-of-the-art DE algorithms. From the simulation results, the proposed method showed better searching accuracy and faster convergence speed on various optimization problems. With the observations on comprehensive experimental results of the economic scheduling of shipboard microgrid in different cases, the proposed algorithm can be successfully applied for this problem. Compared with other multi-objective heuristic algorithms, SaCIDE-r has performed more concentrated Pareto front and faster convergence speed. Meanwhile, both of the fuel cost and the battery cost were minimized. Thus, we may conclude

that, for multi-objective economic scheduling of a shipboard microgrid, SaCIDE-r is a feasible and acceptable solution. In future work, the proposed method needs more verifications on other land-based microgrids with more complicated optimizing objectives.

## REFERENCES

- [1] A. Accetta and M. Pucci, "Energy management system in DC micro-grids of smart ships: Main gen-set fuel consumption minimization and fault compensation," *IEEE Trans. Ind. Appl.*, vol. 55, no. 3, pp. 3097–3113, May/Jun. 2019.
- [2] M. Al-Falahi, T. Tarasiuk, S. Jayasinghe, Z. Jin, H. Enshaei, and J. Guerrero, "AC ship microgrids: Control and power management optimization," *Energies*, vol. 11, no. 6, p. 1458, Jun. 2018.
- [3] S. Castellan, R. Menis, A. Tessarolo, F. Luise, and T. Mazzuca, "A review of power electronics equipment for all-electric ship MVDC power systems," *Int. J. Electr. Power Energy Syst.*, vol. 96, pp. 306–323, Mar. 2018.
- [4] A. García-Olivares, J. Solé, and O. Osychenko, "Transportation in a 100% renewable energy system," *Energy Convers. Manage.*, vol. 158, pp. 266–285, Feb. 2018.
- [5] K. A. Papadogiannis and N. D. Hatziargyriou, "Optimal allocation of primary reserve services in energy markets," *IEEE Trans. Power Syst.*, vol. 19, no. 1, pp. 652–659, Feb. 2004.
- [6] J. M. Guerrero, J. C. Vasquez, J. Matas, M. Castilla, and L. G. de Vicuna, "Control strategy for flexible microgrid based on parallel line-interactive UPS systems," *IEEE Trans. Ind. Electron.*, vol. 56, no. 3, pp. 726–736, Mar. 2009.
- [7] S. Jain and V. Agarwal, "A new algorithm for rapid tracking of approximate maximum power point in photovoltaic systems," *IEEE Power Electron Lett.*, vol. 2, no. 1, pp. 16–19, Mar. 2004.
- [8] K.-J. Lee, D. Shin, D.-W. Yoo, H.-K. Choi, and H.-J. Kim, "Hybrid photovoltaic/diesel green ship operating in standalone and grid-connected mode—Experimental investigation," *Energy*, vol. 49, pp. 475–483, Jan. 2013.
- [9] O. Krishan and S. Suhag, "Techno-economic analysis of a hybrid renewable energy system for an energy poor rural community," *J. Energy Storage*, vol. 23, pp. 305–319, Jun. 2019.
- [10] S. Mandal, B. K. Das, and N. Hoque, "Optimum sizing of a stand-alone hybrid energy system for rural electrification in bangladesh," *J. Cleaner Prod.*, vol. 200, pp. 12–27, Nov. 2018.
- [11] J. Vishnupriyan and P. S. Manoharan, "Prospects of hybrid photovoltaic–diesel standalone system for six different climate locations in indian state of tamil nadu," *J. Cleaner Prod.*, vol. 185, pp. 309–321, Jun. 2018.
- [12] C. Brandoni and B. Bošnjaković, "HOMER analysis of the water and renewable energy nexus for water-stressed urban areas in sub-saharan africa," *J. Cleaner Prod.*, vol. 155, pp. 105–118, Jul. 2017.
- [13] S. A. Shezan, S. Julai, M. A. Kibria, K. R. Ullah, R. Saidur, W. T. Chong, and R. K. Akikur, "Performance analysis of an off-grid wind-PV (photovoltaic)-diesel-battery hybrid energy system feasible for remote areas," *J. Cleaner Prod.*, vol. 125, pp. 121–132, Jul. 2016.
- [14] A. Y. Hatata, G. Osman, and M. M. Aladl, "An optimization method for sizing a solar/wind/battery hybrid power system based on the artificial immune system," *Sustain. Energy Technol. Assessments*, vol. 27, pp. 83–93, Jun. 2018.
- [15] M. J. H. Moghaddam, A. Kalam, S. A. Nowdeh, A. Ahmadi, M. Babanezhad, and S. Saha, "Optimal sizing and energy management of stand-alone hybrid photovoltaic/wind system based on hydrogen storage considering LOEE and LOLE reliability indices using flower pollination algorithm," *Renew. Energy*, vol. 135, pp. 1412–1434, May 2019.
- [16] S. S. Singh and E. Fernandez, "Modeling, size optimization and sensitivity analysis of a remote hybrid renewable energy system," *Energy*, vol. 143, pp. 719–731, Jan. 2018.
- [17] O. Ekren and B. Y. Ekren, "Size optimization of a PV/wind hybrid energy conversion system with battery storage using simulated annealing," *Appl. Energy*, vol. 87, no. 2, pp. 592–598, Feb. 2010.
- [18] W. Zhang, A. Maleki, and M. A. Rosen, "A heuristic-based approach for optimizing a small independent solar and wind hybrid power scheme incorporating load forecasting," *J. Cleaner Prod.*, vol. 241, Dec. 2019, Art. no. 117920.
- [19] A. Maleki, "Modeling and optimum design of an off-grid PV/WT/FC/diesel hybrid system considering different fuel prices," *Int. J. Low-Carbon Technol.*, vol. 13, no. 2, pp. 140–147, Jun. 2018.
- [20] A. Maleki and F. Pourfayaz, "Optimal sizing of autonomous hybrid photovoltaic/wind/battery power system with LPSP technology by using evolutionary algorithms," *Sol. Energy*, vol. 115, pp. 471–483, May 2015.
- [21] B. Wu, A. Maleki, F. Pourfayaz, and M. A. Rosen, "Optimal design of stand-alone reverse osmosis desalination driven by a photovoltaic and diesel generator hybrid system," *Sol. Energy*, vol. 163, pp. 91–103, Mar. 2018.
- [22] G. Zhang, B. Wu, A. Maleki, and W. Zhang, "Simulated annealing-chaotic search algorithm based optimization of reverse osmosis hybrid desalination system driven by wind and solar energies," *Sol. Energy*, vol. 173, pp. 964–975, Oct. 2018.
- [23] S. Fang, Y. Xu, Z. Li, T. Zhao, and H. Wang, "Two-step multi-objective management of hybrid energy storage system in all-electric ship microgrids," *IEEE Trans. Veh. Technol.*, vol. 68, no. 4, pp. 3361–3373, Apr. 2019.
- [24] A. Anvari-Moghaddam, T. Dragicevic, L. Meng, B. Sun, and J. M. Guerrero, "Optimal planning and operation management of a ship electrical power system with energy storage system," in *Proc. 42nd Annu. Conf. IEEE Ind. Electron. Soc. (IECON)*, Oct. 2016, pp. 2095–2099.
- [25] G. S. Misyris, A. Marinopoulos, D. I. Doukas, T. Tengnér, and D. P. Labridis, "On battery state estimation algorithms for electric ship applications," *Electr. Power Syst. Res.*, vol. 151, pp. 115–124, Oct. 2017.
- [26] M. Nemati, M. Braun, and S. Tenbohlen, "Optimization of unit commitment and economic dispatch in microgrids based on genetic algorithm and mixed integer linear programming," *Appl. Energy*, vol. 210, pp. 944–963, Jan. 2018.
- [27] R. Mallol-Poyato, S. Jiménez-Fernández, P. Díaz-Villar, and S. Salcedo-Sanz, "Adaptive nesting of evolutionary algorithms for the optimization of microgrid's sizing and operation scheduling," *Soft Comput.*, vol. 21, no. 17, pp. 4845–4857, Sep. 2017.
- [28] B. Zhao, H. Qiu, R. Qin, X. Zhang, W. Gu, and C. Wang, "Robust optimal dispatch of AC/DC hybrid microgrids considering generation and load uncertainties and energy storage loss," *IEEE Trans. Power Syst.*, vol. 33, no. 6, pp. 5945–5957, Nov. 2018.
- [29] M. Saffari, M. S. Misaghian, M. Kia, A. Heidari, D. Zhang, P. Dehghanian, and J. Aghaei, "Stochastic robust optimization for smart grid considering various arbitrage opportunities," *Electr. Power Syst. Res.*, vol. 174, Sep. 2019, Art. no. 105847.
- [30] M. A. Hossain, H. R. Pota, S. Squartini, F. Zaman, and J. M. Guerrero, "Energy scheduling of community microgrid with battery cost using particle swarm optimisation," *Appl. Energy*, vol. 254, Nov. 2019, Art. no. 113723.
- [31] H. Shuai, J. Fang, X. Ai, Y. Tang, J. Wen, and H. He, "Stochastic optimization of economic dispatch for microgrid based on approximate dynamic programming," *IEEE Trans. Smart Grid*, vol. 10, no. 3, pp. 2440–2452, May 2019.
- [32] R. Storn and K. Price, "Differential evolution—A simple and efficient heuristic for global optimization over continuous spaces," *J. Global Optim.*, vol. 11, no. 4, pp. 341–359, Dec. 1997.
- [33] C. Wang, Y. Liu, Y. Chen, and Y. Wei, "Self-adapting hybrid strategy particle swarm optimization algorithm," *Soft Comput.*, vol. 20, no. 12, pp. 4933–4963, Dec. 2016.
- [34] C. Wang, Y. Liu, Q. Zhang, H. Guo, X. Liang, Y. Chen, M. Xu, and Y. Wei, "Association rule mining based parameter adaptive strategy for differential evolution algorithms," *Expert Syst. Appl.*, vol. 123, pp. 54–69, Jun. 2019.
- [35] S. Das and P. N. Suganthan, "Differential evolution: A survey of the state-of-the-art," *IEEE Trans. Evol. Comput.*, vol. 15, no. 1, pp. 4–31, Feb. 2011.
- [36] S. Das, S. S. Mullick, and P. N. Suganthan, "Recent advances in differential evolution—An updated survey," *Swarm Evol. Comput.*, vol. 27, pp. 1–30, Apr. 2016.
- [37] Y. Wang, Z. Cai, and Q. Zhang, "Differential evolution with composite trial vector generation strategies and control parameters," *IEEE Trans. Evol. Comput.*, vol. 15, no. 1, pp. 55–66, Feb. 2011.
- [38] R. Mallipeddi, P. N. Suganthan, Q. K. Pan, and M. F. Tasgetiren, "Differential evolution algorithm with ensemble of parameters and mutation strategies," *Appl. Soft Comput.*, vol. 11, no. 2, pp. 1679–1696, Mar. 2011.
- [39] S. M. Islam, S. Das, S. Ghosh, S. Roy, and P. N. Suganthan, "An adaptive differential evolution algorithm with novel mutation and crossover strategies for global numerical optimization," *IEEE Trans. Syst., Man, Cybern. B, Cybern.*, vol. 42, no. 2, pp. 482–500, Apr. 2012.
- [40] W. Gong and Z. Cai, "Differential evolution with ranking-based mutation operators," *IEEE Trans. Cybern.*, vol. 43, no. 6, pp. 2066–2081, Dec. 2013.

- [41] G. Wu, R. Mallipeddi, P. N. Suganthan, R. Wang, and H. Chen, "Differential evolution with multi-population based ensemble of mutation strategies," *Inf. Sci.*, vol. 329, pp. 329–345, Feb. 2016.
- [42] S. Birolgil, "Hybrid harris hawk optimization based on differential evolution (HHODE) algorithm for optimal power flow problem," *IEEE Access*, vol. 7, pp. 184468–184488, 2019.
- [43] C. Wang, Y. Liu, X. Liang, H. Guo, Y. Chen, and Y. Zhao, "Self-adaptive differential evolution algorithm with hybrid mutation operator for parameters identification of PMSM," *Soft Comput.*, vol. 22, no. 4, pp. 1263–1285, Feb. 2018.
- [44] T. Li and H. Dong, "Unsupervised feature selection and clustering optimization based on improved differential evolution," *IEEE Access*, vol. 7, pp. 140438–140450, 2019.
- [45] H. Tian, M. Shuai, and K. Li, "Optimization study of line planning for high speed railway based on an improved multi-objective differential evolution algorithm," *IEEE Access*, vol. 7, pp. 137731–137743, 2019.
- [46] L. Zhang, T.-T. Liu, F.-Q. Wen, L. Hu, C. Hei, and K. Wang, "Differential evolution based regional coverage-enhancing algorithm for directional 3D wireless sensor networks," *IEEE Access*, vol. 7, pp. 93690–93700, 2019.
- [47] S. Wang, L. Yu, L. Wu, Y. Dong, and H. Wang, "An improved differential evolution algorithm for optimal location of battery swapping stations considering multi-type electric vehicle scale evolution," *IEEE Access*, vol. 7, pp. 73020–73035, 2019.
- [48] Y. Li, B. Hu, X. Zheng, and X. Li, "EEG-based mild depressive detection using differential evolution," *IEEE Access*, vol. 7, pp. 7814–7822, 2019.
- [49] J.-H. Zhang, Y. Zhang, and Y. Zhou, "Path planning of mobile robot based on hybrid multi-objective bare bones particle swarm optimization with differential evolution," *IEEE Access*, vol. 6, pp. 44542–44555, 2018.
- [50] M. G. Villarreal-Cervantes, A. Rodriguez-Molina, C.-V. Garcia-Mendoza, O. Penalosa-Mejia, and G. Sepulveda-Cervantes, "Multi-objective on-line optimization approach for the DC motor controller tuning using differential evolution," *IEEE Access*, vol. 5, pp. 20393–20407, 2017.
- [51] D. W. Palmer, M. Kirschenbaum, J. Murton, R. Vaidyanathan, and R. D. Quinn, "Development of collective control architectures for small quadruped robots based on human swarming behavior," in *Proc. 2nd Int. Workshop Math. Algorithms Social Insects*, 2010, pp. 123–130.
- [52] L. M. Zheng, S. X. Zhang, K. S. Tang, and S. Y. Zheng, "Differential evolution powered by collective information," *Inf. Sci.*, vol. 399, pp. 13–29, Aug. 2017.
- [53] M. C. Schut, "On model design for simulation of collective intelligence," *Inf. Sci.*, vol. 180, no. 1, pp. 132–155, Jan. 2010.
- [54] M. Avlonitis, I. Karydis, and S. Sioutas, "Early prediction in collective intelligence on video users' activity," *Inf. Sci.*, vol. 298, pp. 315–329, Mar. 2015.
- [55] D. K. Jha, P. Chattopadhyay, S. Sarkar, and A. Ray, "Path planning in GPS-denied environments via collective intelligence of distributed sensor networks," *Int. J. Control.*, vol. 89, no. 5, pp. 984–999, May 2016.
- [56] K. Täuscher, "Leveraging collective intelligence: How to design and manage crowd-based business models," *Bus. Horizons*, vol. 60, no. 2, pp. 237–245, Mar. 2017.
- [57] S. G. de-los-Cobos-Silva, R. A. Mora-Gutiérrez, M. A. Gutiérrez-Andrade, E. A. Rincón-García, A. Ponsich, and P. Lara-Velázquez, "Development of seven hybrid methods based on collective intelligence for solving nonlinear constrained optimization problems," *Artif. Intell. Rev.*, vol. 49, no. 2, pp. 245–279, Feb. 2018.
- [58] B. Yang, T. Yu, X. Zhang, H. Li, H. Shu, Y. Sang, and L. Jiang, "Dynamic leader based collective intelligence for maximum power point tracking of PV systems affected by partial shading condition," *Energy Convers. Manage.*, vol. 179, pp. 286–303, Jan. 2019.
- [59] F. Petrillo, Y.-G. Guéhéneuc, M. Pimenta, C. D. S. Freitas, and F. Khomh, "Swarm debugging: The collective intelligence on interactive debugging," *J. Syst. Softw.*, vol. 153, pp. 152–174, Jul. 2019.
- [60] B. S. Borowy and Z. M. Salameh, "Optimum photovoltaic array size for a hybrid wind/PV system," *IEEE Trans. Energy Convers.*, vol. 9, no. 3, pp. 482–488, Sep. 1994.
- [61] X. Luo, J. Wang, M. Dooner, and J. Clarke, "Overview of current development in electrical energy storage technologies and the application potential in power system operation," *Appl. Energy*, vol. 137, pp. 511–536, Jan. 2015.
- [62] M. Motavasel, A. R. Seifi, and T. Niknam, "Multi-objective energy management of CHP (combined heat and power)-based micro-grid," *Energy*, vol. 51, pp. 123–136, Mar. 2013.
- [63] J. Feng, J. Zhang, C. Wang, and M. Xu, "Self-adaptive collective intelligence-based mutation operator for differential evolution algorithms," *J. Supercomput.*, vol. 76, no. 2, pp. 876–896, Feb. 2020.
- [64] J. Brest, S. Greiner, B. Boskovic, M. Mernik, and V. Zumer, "Self-adapting control parameters in differential evolution: A comparative study on numerical benchmark problems," *IEEE Trans. Evol. Comput.*, vol. 10, no. 6, pp. 646–657, Dec. 2006.
- [65] A. Maleki, "Design and optimization of autonomous solar-wind-reverse osmosis desalination systems coupling battery and hydrogen energy storage by an improved bee algorithm," *Desalination*, vol. 435, pp. 221–234, Jun. 2018.
- [66] A. K. Qin, V. L. Huang, and P. N. Suganthan, "Differential evolution algorithm with strategy adaptation for global numerical optimization," *IEEE Trans. Evol. Comput.*, vol. 13, no. 2, pp. 398–417, Apr. 2009.
- [67] J. Zhang and A. C. Sanderson, "JADE: Adaptive differential evolution with optional external archive," *IEEE Trans. Evol. Comput.*, vol. 13, no. 5, pp. 945–958, Oct. 2009.
- [68] W. Gong, Á. Fialho, Z. Cai, and H. Li, "Adaptive strategy selection in differential evolution for numerical optimization: An empirical study," *Inf. Sci.*, vol. 181, no. 24, pp. 5364–5386, Dec. 2011.
- [69] J. Derrac, S. García, D. Molina, and F. Herrera, "A practical tutorial on the use of nonparametric statistical tests as a methodology for comparing evolutionary and swarm intelligence algorithms," *Swarm Evol. Comput.*, vol. 1, no. 1, pp. 3–18, Mar. 2011.
- [70] S. García, A. Fernández, J. Luengo, and F. Herrera, "Advanced non-parametric tests for multiple comparisons in the design of experiments in computational intelligence and data mining: Experimental analysis of power," *Inf. Sci.*, vol. 180, no. 10, pp. 2044–2064, May 2010.
- [71] B. Qian, L. Wang, D.-X. Huang, W.-L. Wang, and X. Wang, "An effective hybrid DE-based algorithm for multi-objective flow shop scheduling with limited buffers," *Comput. Oper. Res.*, vol. 36, no. 1, pp. 209–233, Jan. 2009.
- [72] S. Salcedo-Sanz, D. Manjarrés, Á. Pastor-Sánchez, J. Del Ser, J. A. Portilla-Figueras, and S. Gil-López, "One-way urban traffic reconfiguration using a multi-objective harmony search approach," *Expert Syst. Appl.*, vol. 40, no. 9, pp. 3341–3350, Jul. 2013.
- [73] K. Deb, A. Pratap, S. Agarwal, and T. Meyarivan, "A fast and elitist multiobjective genetic algorithm: NSGA-II," *IEEE Trans. Evol. Comput.*, vol. 6, no. 2, pp. 182–197, Apr. 2002.



**JINHONG FENG** received the B.Sc. and M.Sc. degrees in marine engineering from Dalian Maritime University, Dalian, China, in 2007 and 2009, respectively, where he is currently pursuing the Ph.D. degree in marine engineering. He is also a Lecturer with the Marine Engineering College. His current research interests include marine engineering automation and control, differential evolution algorithm, artificial intelligence, and smart ship.



**JUNDONG ZHANG** received the B.Sc., M.Sc., and D.Sc. degrees in marine engineering from Dalian Maritime University, Dalian, China, in 1989, 1992, and 1998, respectively. He is currently a Full Professor with Dalian Maritime University. His research interests include marine engineering automation and control, integrated supervision, application of computer and networks, marine engineering education, and electrical system design.



**CHUAN WANG** received the M.S. and Ph.D. degrees in marine engineering from the Marine Engineering College, Dalian Maritime University, China, in 2009 and 2012, respectively. He is currently an Associate Professor with the Marine Engineering College, Dalian Maritime University. His current research interests include automation of electric power systems, optimization methods, and triboelectric nanogenerators.



**RUIZHENG JIANG** received the B.Sc. and M.Sc. degrees in marine engineering from Dalian Maritime University, Dalian, China, in 2007 and 2009, respectively, where he is currently pursuing the Ph.D. degree in marine engineering. He is also a Lecturer with the Marine Engineering College, Dalian Maritime University. His current research interests include simulation of marine power systems, optimization methods, artificial intelligence, and smart ship.



**MINGYI XU** received the Ph.D. degree from Peking University, in 2012. From 2016 to 2017, he was with the Professor Zhong Lin Wang's Group, Georgia Institute of Technology. He is currently a Full Professor with the Marine Engineering College, Dalian Maritime University. His current research interests include blue energy, self-powered systems, and triboelectric nanogenerators and its practical applications in smart ship and ocean.

• • •